International Journal of Thermal Sciences 88 (2015) 47–58

Contents lists available at ScienceDirect

International Journal of Thermal Sciences

journal homepage: www.elsevier.com/locate/ijts

Analytical solution of discontinuous heat extraction for sustainability and recovery aspects of borehole heat exchangers

Selçuk Erol [1], Mir Amid Hashemi [1], Bertrand François*

Université Libre de Bruxelles (ULB), Building, Architecture and Town Planning Dept (BATir), Laboratoire de GéoMécanique, Avenue F.D. Roosevelt, 50 – CPI 194/2, B – 1050 Bruxelles, Belgium

ARTICLE INFO

Article history:
Received 13 September 2013
Received in revised form
27 August 2014
Accepted 13 September 2014
Available online

Keywords:
Ground source heat pump
Analytical solution
Discontinuous heat extraction
Conduction
Advection
Dispersion

ABSTRACT

Existing analytical solutions for thermal analysis of ground source heat pump (GSHP) systems evaluate temperature change in the carrier-fluid and the surrounding ground in the production period of a single borehole heat exchanger (BHE) only if a continuous heat load is assigned. In the present study, we modified the Green's function, which is the solution of heat conduction/advection/dispersion equation in porous media, for discontinuous heat extraction by analytically convoluting rectangular function or pulses in time domain both for single and multi-BHEs field. The adapted analytical models for discontinuous heat extraction are verified with numerical finite element code. The comparison results agree well with numerical results both for conduction and advection dominated heat transfer systems, and analytical solutions provide significantly shorter runtime compared to numerical simulations (approx. 1500 times shorter). Furthermore, we investigated the sustainability and recovery aspects of GSHP systems by using proposed analytical models under different hydro-geological conditions. According to the engineering guideline VDI 4640, a linear relationship between thermal conductivity of the ground and the sustainable heat extraction rate is demonstrated for multi-BHEs.

1. Introduction

GSHPs are known as renewable and sustainable energy systems for decades [1–7]. In order to keep the performance of these systems suitable in decades, a proper installation should be planned for BHE, and to re-operate them after an operation period, the ground needs time to recover from temperature drop. This is particularly the case for multi-BHEs that may affect significantly the ground temperature on a relatively large area.

Rybach and Eugster [3] carried out 2D numerical studies on the sustainability and renewability aspects of a single BHE in a long-term performance in Switzerland. The first 11 years operation of a BHE, measured data are set as the load profile of heat extraction, and an additional load profile of 19 years is extrapolated according to the meteorological data. They showed the temperature decrease in the ground at different distances apart from the BHE at the depth of 50 m during the production period of 30 years and subsequent 30 years as the recovery phase of the ground. According to their results, during the production period the temperature change of the ground was not less than ~7 K at the distance of 0.3 m, and when the operation is stopped, the ground is quickly recovered in several years (e.g. Temperature change of the ground = ~1 K), and after the recovery phase of 30 years the temperature drop was nearly 0.1 K regarding to undisturbed ground temperature. Signorelli [4] investigated the sustainability of BHEs with 3D numerical studies for both a single and multi-BHEs (6 BHEs, array spacing between 3 and 15 m). The temperature change at 50 m depth and 0.1 m distance from the BHE was less than 0.1 K after a 70 years recovery period for multi-BHE field with the array spacing of 7.5 m, whereas after 24 years for a single BHE. Lazzari et al. [8] studied on the long-term performance of single and multi-BHEs field with periodic (sinusoidal) heat load only in a conduction dominated heat transfer system under the consideration of two different ground thermal conductivity. Particularly, they pointed out that even with a large space distance between BHEs (14 m), the full compensation of the ground temperature is needed in case of multi-BHEs field (i.e. in winter heating, in summer cooling). Furthermore, such a similar study under groundwater flow is carried out by Zanchini et al. [9]. They showed that with increasing of Péclet number (proportional to the groundwater flow), the performance of BHEs field becomes more sustainable.

* Corresponding author. Tel.: +32 2 650 27 35; fax: +32 2 650 27 43.
E-mail addresses: selcuk.erol@ulb.ac.be (S. Erol), mihashem@ulb.ac.be (M.A. Hashemi), bertrand.francois@ulb.ac.be (B. François).
[1] Tel.: +32 2 650 27 46.

http://dx.doi.org/10.1016/j.ijthermalsci.2014.09.007
1290-0729/

Nomenclature

a	thermal diffusivity (m^2/s)
c	specific heat capacity (J/kg/K)
H	borehole length (m)
Q_P	energy extraction or injection (J)
Q_L	heat input per meter depth (J/m)
q_L	heat input rate per unit length of borehole (W/m)
t	time (s)
T	temperature (K)
v_T	thermal transport velocity (m/s)
u_x	darcy's velocity (m/s)
x, y, z	space coordinates (m)

Greek symbols

α_l	longitudinal thermal dispersion coefficient
α_t	transversal thermal dispersion coefficient
λ_m	bulk thermal conductivity of porous medium (W/m/K)
λ_x	effective thermal conductivity in the longitudinal direction (W/m/K)
$\lambda_y = \lambda_z$	effective thermal conductivity in the transverse direction (W/m/K)
ρ	density (kg/m^3)

Subscripts

m	medium
w	water

Those previous studies already showed that GSHP systems provide reliable performance and can be used as renewable energy source. However, this is validated only for one-type of geology. In a long-term operation of a BHE, the sustainable heat extraction and the ground temperature recover after the operation depend on hydro-geological and thermo-physical characteristics of the ground.

In order to investigate the scenarios mentioned above with recovery periods of BHEs after an operation, current appropriate methods are to evaluate temperature change in the ground with numerical studies. However, the numerical simulations of GSHP systems are 3D problem and if the discontinuous operation is taken into account, it requires powerful computers due to large computational effort. On the other hand, most of the analytical solutions described in literature consider a constant continuous heat extraction/injection in time merely for a single BHE [10–16], or discontinuous heat extraction under different conditions [10,17,18]. Eskilson [10] described a simple analytical solution for discontinuous heat extraction neglecting three-dimensional effect, but his equation provides only sinusoidal oscillations of temperature signal depending on the assigned distance apart from a single source. Claesson and Eskilson [17] presented 1D analytical solution of a finite line heat source to analyze dimensionless temperature change of subsurface for single pulse, and pulsated heat extraction rate. The temperature solution is obtained for any piecewise constant heat extraction value by superposition using Duhamel's theorem [19]. In case of multiple heat sources, Claesson and Probert [20] derived an analytical solution for temperature field of heat releasing canisters containing nuclear waste. The local field temperature is solved with a finite line heat source and infinite grid of point sources. The solutions for different heat sources are superimposed. Recently, the long-term performance of BHEs field has been investigated with an analytical solution that is extended for sinusoidally varying heat load in an infinite medium neglecting the groundwater flow [21].

The main objective of this study is to obtain an analytical solution to evaluate temperature change in the ground both for single and multi-BHEs that considers discontinuous heat extraction, thermal conduction, advection and dispersion. We start from the Green's function which is the solution of heat conduction/advection/dispersion equation in porous media and apply an analytical convolution of that function with a rectangular function or pulses, which have different period lengths and pulse heights. The evolution of the mean fluid temperature of the carrying fluid to maintain a constant heat extraction rate is evaluated along the time. Temperature evaluation in the surrounding ground is also deduced. The developed equation is verified with the finite element software COMSOL Multiphysics. Furthermore, the sustainability of single/multi-BHEs under different hydro-geological conditions is investigated with analytical solution to model 30 years production period, and also from an environmental point of view, the recovery period after those 30 years of operation is studied.

2. Analytical solution for discontinuous heat extraction

2.1. Single BHE

In geothermal literature, the existing finite and cylindrical analytical solutions with a constant heat load may provide satisfactory estimation of ground thermal parameters to design GSHP systems [22–24]. In a real case, the GSHP systems can be operated with various periods in a given time for different heat extraction/injection rates, instead of a continuous operation as assumed by most of other previously presented analytical methods. Some authors evaluated the temperature change for thermal response test operation in the vicinity of a single BHE or BHE field with an analytical solution by using multiple load aggregation algorithms [25–30]. However, some of those approaches may not be appropriate in all cases to evaluate the accurate temperature change in the ground due to neglecting axial effect, considering only single BHE or not taking into account groundwater flow. In particular when Darcy's velocity in porous media is considered, the thermal dispersion coefficients must be taken into account, because thermal dispersion has a large impact on the distribution of the temperature plume around BHE, for Darcy's velocity larger than 10^{-8} m/s [31].

The governing equation of the heat conduction/advection/dispersion in porous media is given as follows:

$$\rho_m c_m \frac{\partial T}{\partial t} = \left(\lambda_x \frac{\partial^2 T}{\partial x^2} + \lambda_y \frac{\partial^2 T}{\partial y^2} + \lambda_z \frac{\partial^2 T}{\partial z^2} \right) - u_x \rho_w c_w \frac{\partial T}{\partial x} + s \tag{1}$$

in which u_x is the Darcy's velocity on the x-direction, s is a volumetric heat source, and $\rho_m c_m$ is the volumetric heat capacity of the medium, which can be calculated as the weighted arithmetic mean of the solids $\rho_s c_s$ and volumetric heat capacity of water $\rho_w c_w$ [32]:

$$\rho_m c_m = (1 - n)\rho_s c_s + n \rho_w c_w \tag{2}$$

where n is the porosity.

The components of effective longitudinal and transverse thermal conductivities are defined on the directions of x, y and z as follows [33,34]:

$$\lambda_x = \lambda_m + \alpha_l \rho_w c_w u_x \tag{3}$$

$$\lambda_y = \lambda_z = \lambda_m + \alpha_t \rho_w c_w u_x \tag{4}$$

where λ_m is the bulk thermal conductivity of porous medium in the absence of groundwater flow, α_l and α_t are the longitudinal and

transverse dispersivities, respectively. The thermal dispersion is a linear function of groundwater flow and relates to the anisotropy of the velocity field [31,35]. The thermal dispersion coefficients depend on different components of porous media (e.g., Darcy's velocity, particle size of the media, field scale). In the literature, some empirical relationships can be found to calculate the thermal dispersion coefficients [36–38]. The complete determination of those two parameters (α_l and α_t) is out of the scope of the present study. Consequently, mean representative values have been taken for the computations.

The solution of the partial differential equation for heat transfer in porous media (Eq. (1)) is obtained from the Green's function G of a pulse point source Q_P at the given point coordinates (x', y', z') and time $t = 0$ [39]:

$$\Delta T(x,y,z,t) = \frac{G(x,y,z,t)}{\rho_m c_m} = \frac{Q_P}{8\rho_m c_m \sqrt{\lambda_x\lambda_y\lambda_z}\left(\frac{\pi t}{\rho_m c_m}\right)^{3/2}} \times \exp\left[-\frac{(x-x')^2}{\frac{4\lambda_x t}{\rho_m c_m}} - \frac{(y-y')^2}{\frac{4\lambda_y t}{\rho_m c_m}} - \frac{(z-z')^2}{\frac{4\lambda_z t}{\rho_m c_m}}\right] \tag{5}$$

In order to take into account the axial effect and the groundwater flow, this solution can be applied for the response of a constant line-source with finite length H along the vertical z direction with a pulse heat extraction after applying moving source theory [19] by integrating Eq. (5) along the z-axis [13]:

$$\Delta T(x,y,z,t) = \frac{Q_L}{8\rho_m c_m \sqrt{\lambda_x\lambda_y\lambda_z}\left(\frac{\pi t}{\rho_m c_m}\right)^{3/2}} \times \int_0^H \exp\left[-\frac{(x-v_T t)^2}{\frac{4\lambda_x t}{\rho_m c_m}} - \frac{y^2}{\frac{4\lambda_y t}{\rho_m c_m}} - \frac{(z-z')^2}{\frac{4\lambda_z t}{\rho_m c_m}}\right] dz' \tag{6}$$

where Q_L is a pulse heat input per meter depth and v_T is thermal transport velocity that can be calculated as follows [16]:

$$v_T = \frac{\mathrm{Pe}\, a}{d} = u_x \frac{\rho_w c_w}{\rho_m c_m} \tag{7}$$

where a is the thermal diffusivity ($\lambda_m/\rho_m c_m$), d is the mean particle size of porous medium and Pe is Péclet number giving as follows:

$$\mathrm{Pe} = \frac{u_x \rho_w c_w d}{\lambda_m} \tag{8}$$

In order to simplify Eq. (6), the exponential function can be integrated by using u-substitution method:

$$\Delta T(x,y,z,t) = \frac{Q_L}{8\rho_m c_m \sqrt{\lambda_x\lambda_y\lambda_z}\left(\frac{\pi t}{\rho_m c_m}\right)^{3/2}} \times \exp\left[-\frac{(x-v_T t)^2}{\frac{4\lambda_x t}{\rho_m c_m}} - \frac{y^2}{\frac{4\lambda_y t}{\rho_m c_m}}\right] \int_0^H \exp\left[-\frac{(z-z')^2}{\frac{4\lambda_z t}{\rho_m c_m}}\right] dz' \tag{9}$$

$$u^2 = \frac{(z-z')^2}{\frac{4\lambda_z t}{\rho_m c_m}} \rightarrow u = \frac{z-z'}{\sqrt{\frac{4\lambda_z t}{\rho_m c_m}}} \tag{10}$$

$$-\sqrt{\frac{4\lambda_z t}{\rho_m c_m}} du = dz' \tag{11}$$

The limits of u-value becomes:

$$u: \frac{z-H}{\sqrt{\frac{4\lambda_z t}{\rho_m c_m}}} \rightarrow \frac{z}{\sqrt{\frac{4\lambda_z t}{\rho_m c_m}}} \tag{12}$$

Substituting Eq. (11) and Eq. (12) into Eq. (9), allows to re-write the equation as:

$$\Delta T(x,y,z,t) = \frac{Q_L}{8\rho_m c_m \sqrt{\lambda_x\lambda_y\lambda_z}\left(\frac{\pi t}{\rho_m c_m}\right)^{3/2}} \exp\left[-\frac{(x-v_T t)^2}{\frac{4\lambda_x t}{\rho_m c_m}} - \frac{y^2}{\frac{4\lambda_y t}{\rho_m c_m}}\right] \int_{\frac{z-H}{\sqrt{\frac{4\lambda_z t}{\rho_m c_m}}}}^{\frac{z}{\sqrt{\frac{4\lambda_z t}{\rho_m c_m}}}} \exp\left(-u^2\right)\left(\sqrt{\frac{4\lambda_z t}{\rho_m c_m}}\right) du \tag{13}$$

The integration of exponential function $f = \exp(-u^2)$ can be expressed with error function:

$$erf(x) = \frac{2}{\sqrt{\pi}} \int_0^x \exp\left(-u^2\right) du \rightarrow \frac{\sqrt{\pi}}{2} erf(x) = \int_0^x \exp\left(-u^2\right) du \tag{14}$$

By taking the integration of exponential function, therefore, Eq. (13) reduces to:

$$\Delta T(x,y,z,t) = \frac{Q_L}{8\rho_m c_m \sqrt{\lambda_x\lambda_y\lambda_z}\left(\frac{\pi t}{\rho_m c_m}\right)^{3/2}} \times \sqrt{\frac{4\lambda_z t}{\rho_m c_m}}\ \frac{\sqrt{\pi}}{2} \exp\left[-\frac{(x-v_T t)^2}{\frac{4\lambda_x t}{\rho_m c_m}} - \frac{y^2}{\frac{4\lambda_y t}{\rho_m c_m}}\right] \times \left[erf\left(\frac{z}{\sqrt{\frac{4\lambda_z t}{\rho_m c_m}}}\right) - erf\left(\frac{z-H}{\sqrt{\frac{4\lambda_z t}{\rho_m c_m}}}\right)\right] \tag{15}$$

with simplification, Eq. (15) can be expressed with the error functions as follows:

$$\Delta T(x,y,z,t) = Q_L \underbrace{\frac{1}{8\pi t\sqrt{\lambda_x\lambda_y}} \exp\left[-\frac{(x-v_T t)^2}{\frac{4\lambda_x t}{\rho_m c_m}} - \frac{y^2}{\frac{4\lambda_y t}{\rho_m c_m}}\right]\left[erf\left(\frac{z}{\sqrt{\frac{4\lambda_z t}{\rho_m c_m}}}\right) - erf\left(\frac{z-H}{\sqrt{\frac{4\lambda_z t}{\rho_m c_m}}}\right)\right]}_{f(x,y,z,t)} \tag{16}$$

To apply a discontinuous injection or extraction of heat in time domain, we convolute analytically Eq. (16) with a single or a series of different rectangular pulses referring to the duration of operations in time. For instance, $f(x, y, z, t)$ function is convoluted with a rectangular heat extraction function $q_L(t)$ defined as follows:

$$q_L(t) = \begin{cases} q_L \text{ for } t \in [0,T] \\ 0 \text{ otherwise} \end{cases} \tag{17}$$

in which T is the period of heat extraction. In this simulation, we assume that the heat source per unit length q_L is independent of the depth.

Illustration of convolution can be seen in Fig. 1.

The convolution of q_L and f function is written as follows:

$$\Delta T(x,y,z,t) = \int_{-\infty}^{\infty} q_L(\tau) f(x,y,z,t-\tau)\mathrm{d}\tau = q_L \int_0^{\mathrm{T}} f(x,y,z,t-\tau)\mathrm{d}\tau \tag{18}$$

$$\Delta T(x,y,z,t) = \sum_{i=0}^{n-1} q_L(i\Delta t) f(x,y,z,t-i\Delta t)\Delta t \tag{19}$$

where n denote the time span, $i\ \Delta t$ is the time delay of each unit impulse, and the delayed and shifted impulse response becomes $q_L(i\ \Delta t)\ f(t-i\ \Delta t)\ \Delta t$.

By using the same method, it is possible to convolute f function with rectangular pulses which have different pulse heights and lengths in given identical time span of f function. Thus, recovery period of the ground can be investigated after a production of a single BHE and the numerical computational effort will be decreased.

2.2. Multi-BHEs

In case of multi-BHEs, analytical solution Eq. (16) can be solved in a sum function (Eq. (20)) depending on the grid coordinates of each line heat source as illustrated in Fig. 2:

$$\Delta T(x,y,z,t) = Q_L \underbrace{\sum_{j=1}^{s} \frac{1}{8\pi\sqrt{\lambda_x\lambda_y}} \frac{1}{t} \exp\left\{-\frac{1}{4a(t-t')}\left[\frac{(x-x_j-v_T t)^2}{\frac{4\lambda_x t}{\rho_m c_m}} + \frac{\left(y-y_j\right)^2}{\frac{4\lambda_y t}{\rho_m c_m}}\right]\right\}\left[erf\left(\frac{z}{\sqrt{\frac{4\lambda_z t}{\rho_m c_m}}}\right) - erf\left(\frac{z-H}{\sqrt{\frac{4\lambda_z t}{\rho_m c_m}}}\right)\right]}_{C(x,y,z,t)} \tag{20}$$

For the analytical evaluation of the convolution integral equation, we discretize both q_L and f functions with a differential of Δt, the convolution as a sum of impulse responses at coordinates (x, y, z) is given as:

in which s represents the number of BHEs. We consider the impact of groundwater flow on each BHE at x direction by taking into account thermal transport velocity v_T.

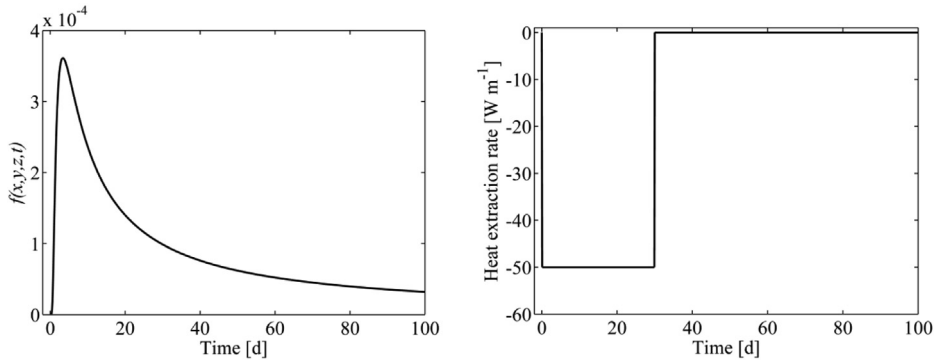

Fig. 1. Illustration of convolution $f(x, y, z, t)$ and q_L heat extraction function in time domain.

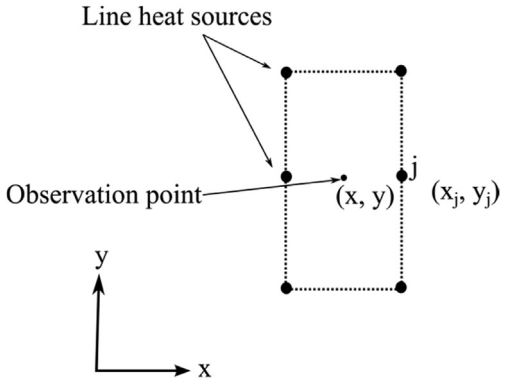

Fig. 2. Illustration of multi-BHEs geometry demonstrating the grid coordinates.

The sum $C(x, y, z, t)$ can be convoluted as described in the previous Section 2.1 to apply discontinuous heat extraction as follows:

$$\Delta T(x,y,z,t) = \sum_{i}^{n-1} q_L(i\Delta t) C(x,y,z,t - i\Delta t)\Delta t \qquad (21)$$

3. Validation

The developed analytical solutions (Eqs. (19) and (21)), for discontinuous heat extraction are verified with 3D numerical models. For the verification, numerical model setup, initial and boundary conditions of the model, input parameters and comparison of the numerical and the analytical solution results are presented in the following.

3.1. Numerical model setup

In order to validate the analytical solution developed above, simple cases for single and multi-BHEs have been considered through numerical models using COMSOL Multiphysics software [40]. The common numerical characteristics are described here for both single and multi-BHEs field models. The study is carried out by a 3D homogeneous model domain (Fig. 3) and BHE is represented with the line heat source(s). A model domain of 40 m × 40 m in the horizontal direction and 60 m in the vertical direction is set for the simulation. The length of line heat source is 50 m for each. The mesh is generated using uniform tetrahedral elements. The single and multi-lines heat sources are centered at the coordinates (0, 0). The coordinates of single and multi-lines heat sources are shown in Fig. 4.

In order to get a better resolution of the temperature variations around the line source, close to it the mesh is further refined along the length of line source and also along the line on which the observation point are placed (at the depth of 25 m).

As the boundary conditions, the load profile of heat extraction with 3 different extraction periods can be seen in Fig. 3. The simulation time is restricted to 160 days in order to maintain runtime in acceptable limits and to avoid large memory allocation of computer. The top of the model surface temperature is fixed to 0 °C, as well as identically assigned initial temperature, to carry out the fulfillment of analytical solution and to observe the relative temperature change in the subsurface. Initial input parameters are given in Table 1. Thermal dispersion is taken into account by imposing anisotropic thermal conductivity of the medium, as described by Eqs. (3) and (4).

The number of elements changes depending on the model of single or multi-lines heat sources (Table 2). For the simulations, the

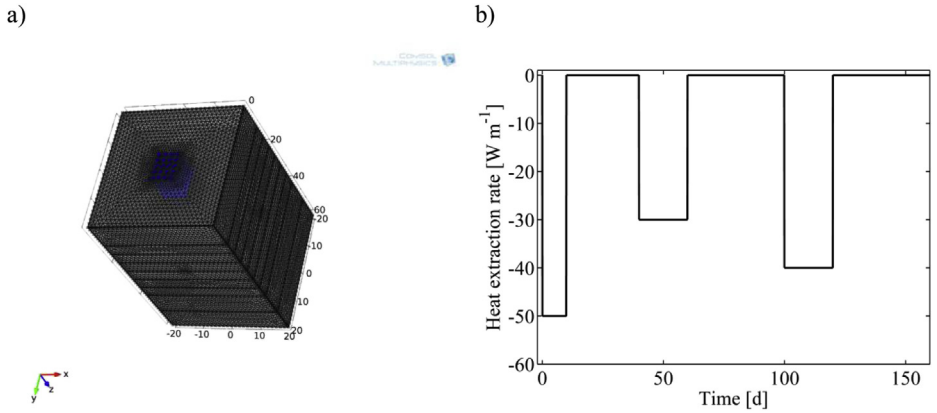

Fig. 3. a) Sketch illustrating 3D model of multi-BHEs field with the line source length of 50 m. b) Load profile of heat extraction.

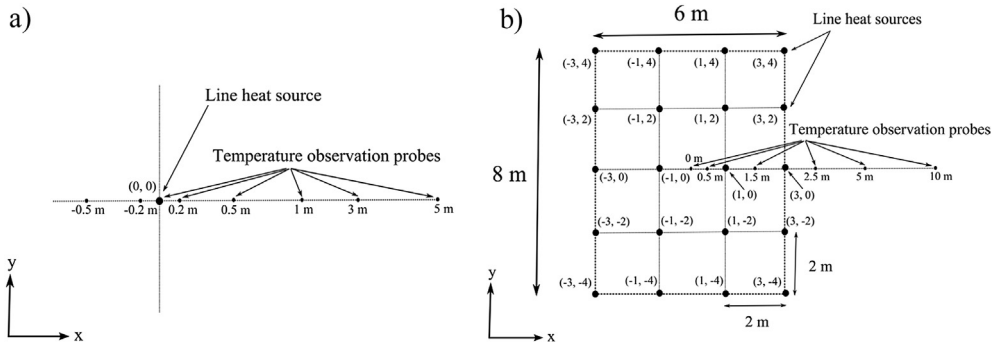

Fig. 4. Illustration of temperature observation points on the *x* direction: a) for single BHE b) for multi-BHEs field. Groundwater flow is set on the *x* direction.

Table 1
Common initial input parameters for the model domain of single and multi-BHEs field.

Parameters	Value
Initial temperature °C (T_o)	0
Bulk thermal conductivity of porous medium W m^{-1} K^{-1} (λ_m)	2.4[a]
Effective thermal conductivity in the longitudinal direction W m^{-1} K^{-1} (λ_x)	6.6[b]
Effective thermal conductivity in the transverse direction W m^{-1} K^{-1} ($\lambda_y = \lambda_z$)	2.82[b]
Volumetric heat capacity MJ m^{-3} K^{-1} ($\rho_m c_m$)	2.8[a]
Groundwater flow/discharge m s^{-1} (u_x)	1×10^{-6}[c]
Longitudinal dispersivity (α_l)	1[d]
Transverse dispersivity (α_t)	0.1[d]

[a] Representative values taken from Ref. [41].
[b] Calculated values according to Eqs. (3) and (4).
[c] Assigned only for the models in which heat advection/dispersion is considered.
[d] Values taken from Ref. [42] to calculate effective thermal conductivities.

basic heat transfer module of COMSOL Multiphysics, which uses Fourier's law, is used, and the groundwater flow is imposed through a homogeneous velocity field. The Backward Euler (Crank-Nicolson Scheme) time marching method with RMS error tolerance of 10^{-3} is applied and the maximum time step interval set to 86,400 s due to better robustness. Table 2 provides a summary of the model setups.

For verification plots, temperature changes are observed in time on the x direction of the coordinate system (Fig. 4).

3.2. Single BHE

The Eq. (19) is solved on MATLAB and compared with the numerical results. According to the results, the analytical method solution agrees well with numerical results both under conduction (Fig. 5) and advection/dispersion (Fig. 6) dominated heat transfer systems (i.e. only water-saturated sand and with the groundwater flow). Comparing the results of temperature difference between conduction and advection/dispersion heat transfer systems, the impact of the groundwater flow/dispersion appears clearly. The first heat extraction phase generates larger temperature decrease in the point located in the x-direction when groundwater flow and dispersion are considered. However, the recovery phase is accelerated due to water flow. Consequently, the subsequent heat extraction induces lower temperature change in the ground close to the BHE. Also, with time, temperature is impacted at larger distance in the direction of the water flow when the groundwater flow and the dispersion are considered (at 10 m, $\Delta T = 0.8$ K with water flow *vs* $\Delta T = 0.2$ K without water flow).

Fig. 7a) and b) depict comparison of temperature contours plotted in the horizontal plan view and vertical cross-section, respectively. The distribution of temperature plume is non-symmetric (pushed forward in the x-direction) due to thermal advection and anisotropic dispersion, both induced by the groundwater movement. Also, the axial effect can be seen on Fig. 7b) close to the beginning and at the end of borehole length.

Table 2
Summary of the model setup for verification.

Parameter	Value
Type of problem	3D
Numerical method for heat transport	Standard Galerkin-FEM
Simulation time	160 days
Number of elements solved for single BHE model/multi BHEs model	834,679/1,975,633
Solver type	Flexible Generalized Minimal Residual method (FGMRES)

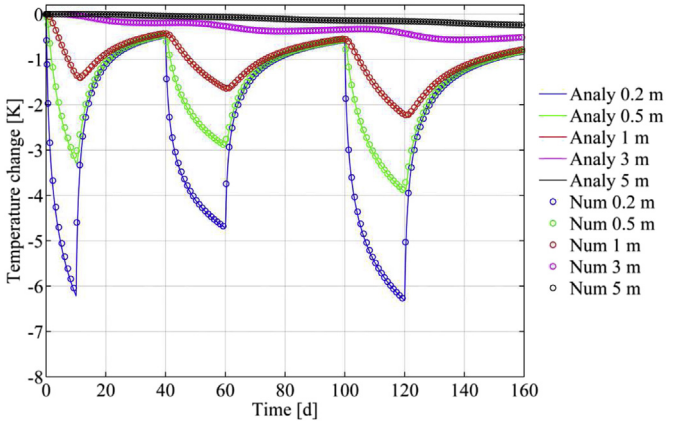

Fig. 5. Comparison of numerical and analytical solution results at the depth of 25 m for single line heat source without groundwater flow. Induced by the load profile of Fig. 3b).

The significant advantage of analytical method can be seen in Table 3. The execution time of Eq. (19) is approximately 1500 times smaller than the runtime of numerical models. Note that, for the analytical solution, the computation time depends on the number of observation point. It has the advantage that it can reduce the calculation time as a function of the amount of required information.

3.3. Multi-BHEs

Eq. (21) is solved on MATLAB and compared with the numerical results. According to the results, again the analytical method solution agrees with numerical results both with (Fig. 9) and without the groundwater flow (Fig. 8). The small discrepancy between the results of advection/dispersion case can be accounted for the mesh discretization of the numerical simulation. The mesh might be finer enough to capture the physics of fluid movement and the anisotropy of the model, but on the other hand it would cause larger computational effort. Comparison of Figs. 8 and 9 shows that the maximum temperature decrease in the ground is substantially reduced by the groundwater flow (from −12 K to −8 K in the simulated case).

Fig. 10a) and b) shows the isotherm contours of temperature difference around multi-BHEs field in conduction and advection dominated heat transfer systems, respectively at 120th day of

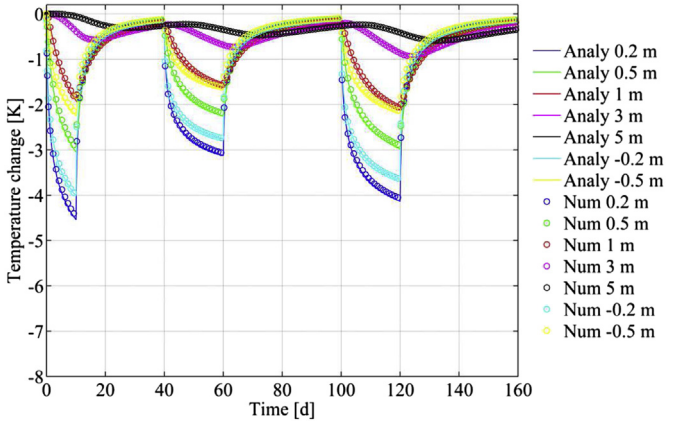

Fig. 6. Comparison of numerical and analytical solution results at the depth of 25 m for single line heat source. Under groundwater flow of 1×10^{-6} m/s on the x-axis direction. Induced by the load profile of Fig. 3b).

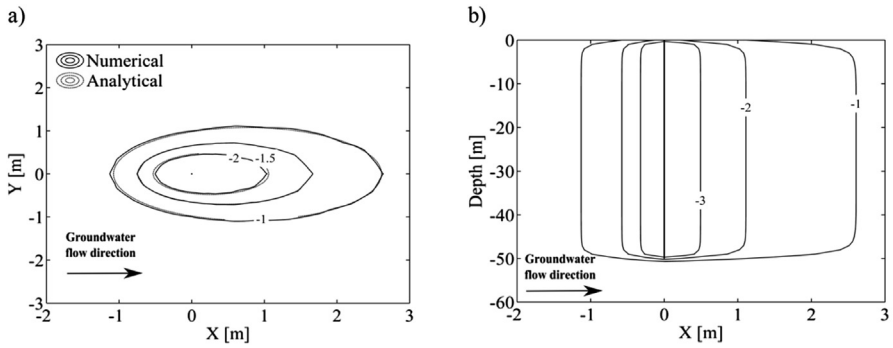

Fig. 7. Relative temperature difference at 120th day for advection under groundwater flow of 1×10^{-6} m/s: a) Comparison between numerical and analytical solution results on plan view at 25 m depth b) Cross section temperature isotherms only for analytical solution.

operation (just after the 3rd cycle of heat extraction). The small comparison difference in Fig. 10b) can be likely accounted for the contour plot interpolation of numerical result when it is exported from COMSOL to MATLAB, because the temperature results are obtained as a text file from the numerical model corresponding to *x* and *y* coordinates.

As shown in Table 4, even in case of multi-BHEs, the analytical solution (Eq. (21)) provides again significantly shorter execution time for the computation of temperature at given observation coordinates. The runtime of analytical solution denotes only for the calculation of assigned number of observation points.

4. Sustainability and recovery aspects

The objective of this section is to investigate the long-term sustainability of single and multiple BHEs under different hydrogeological conditions and subsequent impact of production period on the ground temperature.

Since we validated our analytical solution of discontinuous heat extraction both for single and multi-BHEs, the following studies are carried out with MATLAB by using Eq. (19) and Eq. (21), respectively. In order to estimate an appropriate interval of solutions for such a long-term time span computation, some sensitivity analyses are carried out by comparing the temperature results obtained with different intervals.

4.1. Single BHE

4.1.1. Initial and boundary conditions

Thermal properties of soil and rocks are shown in Table 5. Those underground types are most common geology of the shallow subsurface for northwest Europe. In addition, basalt and granite provide a range of selection due to their low and high thermal conductivity values.

Each type of underground is considered as a scenario. Additionally, in order to investigate the influence of groundwater flow and dispersion on both production and the recovery phases, we included Scenario 2.

As the boundary condition, to set a load profile of heat extraction either into a numerical model or an analytical solution based on a real daily operation causes large computational effort and long runtime due to required small time steps (e.g. <1 h) and allocated memory. It is appropriate to set a constant value during 30 years production period for heat extraction, but the impact of continuous and discontinuous heat extraction must be analyzed (in case, the

Table 3
Comparison of the execution times and time steps for single BHE.

Model	Number of time step[a] (total simulation)	Runtime [sec][a]
Analytical solution (Eq. (19))	2562	9[b]/13[c]
Numerical model 1 no groundwater flow	162	15986
Numerical model 2 with groundwater flow of 1×10^{-6} m/s	162	16974

[a] Hardware specifications: Intel, 4 core i-5 3.10 GHz, RAM: 16 GB.
[b] Calculation for 5 observation points.
[c] Calculation for 7 observation points (Figs. 5 and 6).

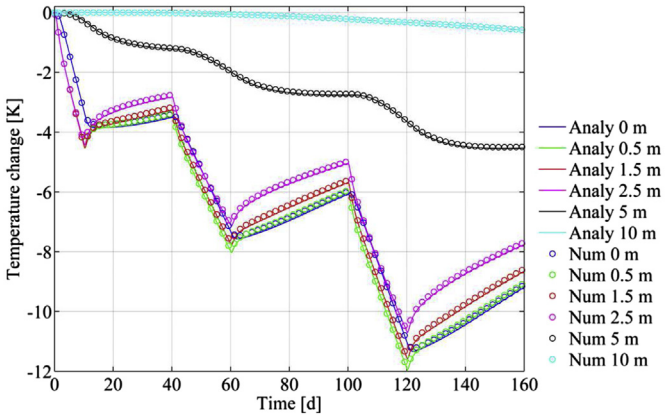

Fig. 8. Comparison of numerical and analytical solution results at the depth of 25 m for multi-BHEs field without groundwater flow.

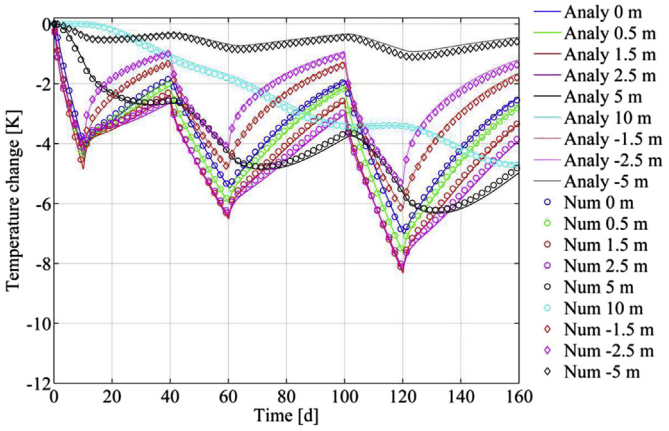

Fig. 9. Comparison of numerical and analytical solution results at the depth of 25 m for multi-BHEs field under groundwater flow of 1×10^{-6} m/s on the *x*-axis direction.

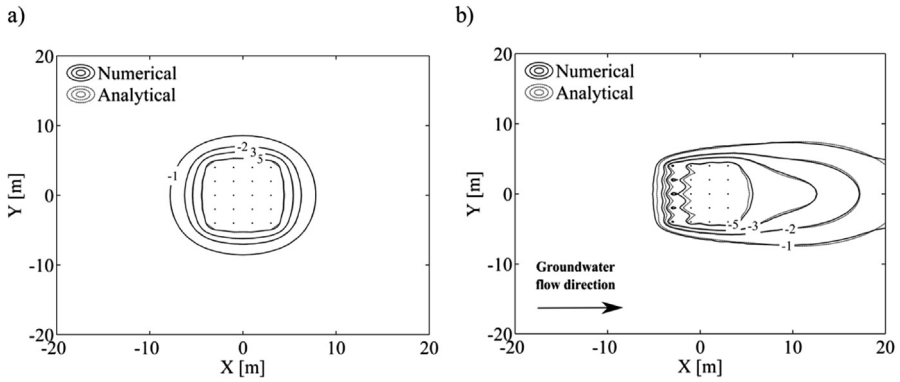

Fig. 10. Comparison of relative temperature difference between numerical and analytical solution results on plan view at 25 m depth at 120th day for multi-BHEs field: a) only water-saturated sand without groundwater flow b) under groundwater flow of 1×10^{-6} m/s.

total amount of heat load must be identical). Signorelli [4] investigated the far-field behavior of BHE for different operation periods with numerical simulations (i.e. single load, multiple load and distributed load profiles). According to climatic data, the operation hours are subdivided to months out of the total 1800 h operation time per year. For instance, the operation is 60 h in September to obtain 300 kWh. Single load denotes 60 h continuous heat extraction and the rest of the month is recovery phase (i.e. 50 W m^{-1} for a BHE with a length of 100 m). The second load profile, called multiple, the BHE is operated 2 h per day, and the rest of 22 h is recovery period. The third load profile represents the total amount of heat extraction, 300 kWh, is distributed to whole month (i.e. ~4.16 W m^{-1} continuous heat extraction). According to Signorelli [4], whatever the load profile is applied the temperature change in the ground is nearly identical after a one year operation (±0.1 K at 0.1 m distance from the BHE). Therefore, we set in our analytical solutions a constant continuous heat extraction of 10.27 W m^{-1} along 30 years operation period for all scenarios (the total amount of heat extraction 9000 kWh per year = 50 W $m^{-1} \times 100$ m $\times$ 1800 h is distributed hourly for a single BHE with a length of 100 m).

Table 4
Comparison of the execution times and time steps for multi-BHEs.

Model	Time step size[a] (total simulation)	Runtime [sec][a]
Analytical solution (Eq. (21))	2562	10[b]/18[c]
Numerical model 1 no groundwater flow	164	13937
Numerical model 2 with groundwater flow of 1×10^{-6} m/s	164	37023

[a] Hardware specifications: Intel, 4 core i-5 3.10 GHz, RAM: 16 GB.
[b] Calculation for 6 observation points.
[c] Calculation for 9 observation points (Figs. 8 and 9).

Table 5
Thermal properties of scenarios.

Scenario	Geology of underground	Thermal conductivity [W m^{-1} K^{-1}]	Bulk volumetric heat capacity of medium [J m^{-3} K^{-1}][a]
1	Water-saturated silica sand	$\lambda_m = 2.4$[a]	2.8×10^6
2	Sand under groundwater flow 1×10^{-6} m/s	$\lambda_x = 6.6$[b], $\lambda_y = \lambda_z = 2.8$[b]	
3	Granite	$\lambda_m = 3.2$[a]	3×10^6
4	Basalt	$\lambda_m = 1.7$[a]	2.5×10^6

[a] Mean values are taken from Ref. [41].
[b] Effective thermal conductivity calculated according to Eqs. (3) and (4).

4.1.2. Results

The relative temperature change results are plotted (e.g. the temperature difference between plume temperature ensuing from the operation and initial ground temperature). Fig. 11 demonstrates that in case of conduction dominated heat transfer system of the ground, temperature drop during the production period increases

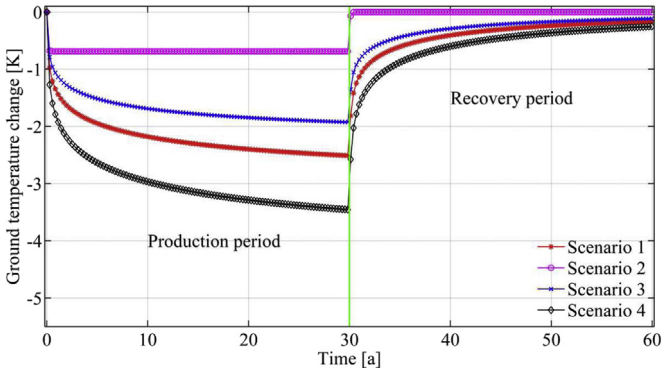

Fig. 11. Comparison results between scenarios. Temperature probes at the depth of 50 m, at the distance from heat line source of 1 m. For Scenario 2, the groundwater flows in the *x* direction.

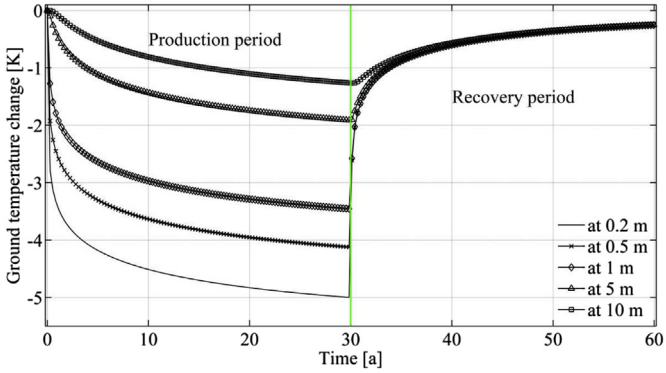

Fig. 12. Temperature probe results of Scenario 4, basalt. Temperature probes at the depth of 50 m from surface.

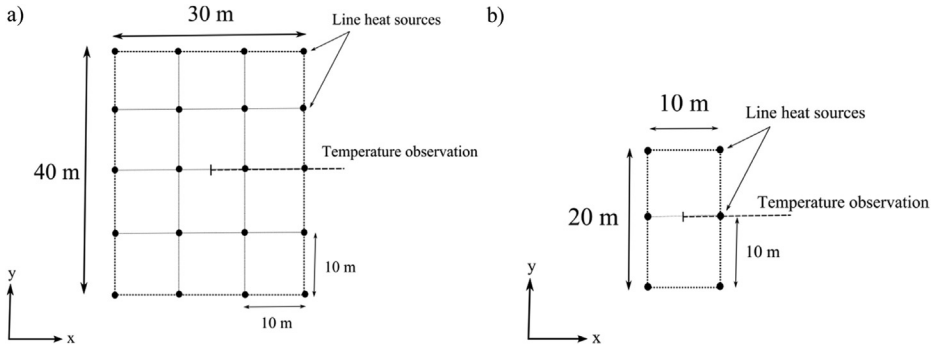

Fig. 13. Geometric arrangement of multi-BHEs field: a) that contains 20 BHEs b) that contains 6 BHEs.

Table 6
Characteristics of the first task scenarios.

Scenario	Number of BHEs with the length of 100 m each	Heat extraction rate [W m^{-1}][a]	Geology	Total amount of heat extraction [W h][a]	Distribution of total amount of heat in a year [W m^{-1}][b]
1	6	65	Granite	2.34×10^8	13.35
2	20			7.02×10^7	
3	6	40	Basalt	1.44×10^8	8.22
4	20			4.32×10^7	

[a] According to VDI 4640 [43] provided minimum values for 1800 h per year for granite and basalt.
[b] Continuous heat extraction 30 years long.

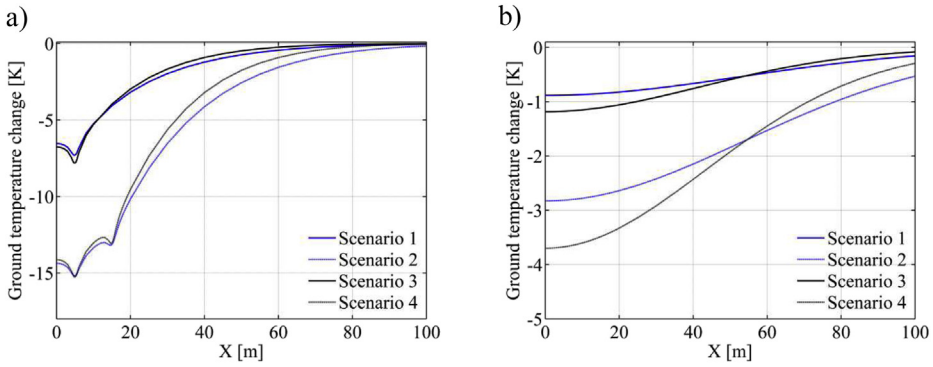

Fig. 14. Comparison of temperature drop of 25 BHEs and 6 BHEs fields over distance at the depth of 50 m with different heat extraction values according to VDI 4640 [43]. a) at the end of 30th year production period b) at the end of 30th year recovery period.

with decreasing thermal properties of ground, but at the end of 30 years recovery period, temperature change of those scenarios is not significant. Referring to the results of scenario 2, the impact of groundwater flow and dispersion ($\alpha_l = 1$ m, $\alpha_t = 0.1$ m) can likely provide more sustainable performance of a BHE during the operation period, and a quick recovery of the ground.

In Fig. 12, when we analyze further the results of scenario 4 due to its lowest thermal properties, even at 10 m distance from the BHE, the mean temperature decrease is nearly 0.5 K in recovery phase. This effect should be taken into account for multi-BHE field, because if considered array distance between BHEs is equal or less than 10 m in poorly conductive ground such as basalt or clay, the performance of the system can be kept sustainable with decreasing the mean fluid temperature, but the impact on the ground temperature would be larger. Therefore, the array distance in a BHE field plays a significant role on the sustainability of heat extraction and the recovery of the ground temperature. In the following section, the far-field behavior of multi-BHEs field results are investigated for proper heat extraction for long-term performance and the impact on the ground temperature after a production period.

4.2. Multi-BHEs field

The study on multi-BHEs field is carried out to determine optimum heat extraction rate for BHEs under different thermo-

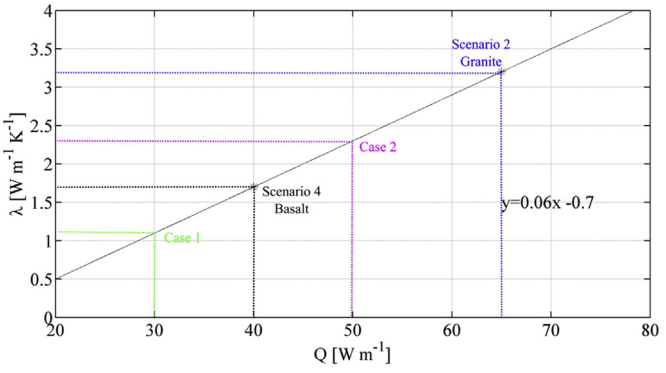

Fig. 15. Best fits for scenario 2 and 4 and corresponding points for Case 1 and Case 2.

Table 7
Characteristics of two generated cases according to correlation in.Fig. 15.

Case	Number of BHEs with the length of 100 m each	Heat extraction rate[a] [W m^{-1}]	Thermal conductivity of the ground [W m^{-1} K^{-1}][a]	Volumetric heat capacity of medium [J m^{-3} K^{-1}][b]	Total amount of heat extraction [W h]	Distribution of total amount of heat in a year [W m^{-1}][c]
1	20	30	1.1	2.5×10^6	1.08×10^8	6.16
2	20	50	2.4	2.8×10^6	1.8×10^8	10.27

[a] Values are provided according the best fit in Fig. 8.
[b] Mean values are taken from Ref. [30] based on correlated the thermal conductivity values, for instance, Case 1 – Clay, Case 2 – water-saturated sand.
[c] Continuous heat extraction 30 years long.

physical conditions of the ground. Therefore, granite and basalt have been chosen for their relatively high difference in thermal conductivity.

4.2.1. Initial and boundary conditions

According to VDI 4640 [43], German guideline for installation and design for GSHP systems, the array distance between BHEs should be at least 6 m with the length of >50 m–100 m, and maximum specific heat extraction rate of 65 W m^{-1} for granite and 40 W m^{-1} for basalt are suggested for an annual operation of 1800 h. These heat extraction values may provide an optimum ground temperature decrease as a function of soil and rock types. The issue is to check whether it is valid also for multiple BHEs field.

We studied on two different fields containing 20 and 6 BHEs, respectively (Fig. 13). The initial thermal parameters of scenarios are set equal ones used in Section 4.1 (Scenario 3 and 4 from Table 5). The groundwater flow/dispersion is neglected for the scenarios considered in this study ($u_x = 0$, $\lambda_m = \lambda_x = \lambda_y = \lambda_z = 0$). The arrays of BHEs are lattice-like square arranged with the space distance of 10 m in x and y directions [44,45]. Total amount of heat extraction value 1800h $\times$ 65 W m^{-1} for granite and $\times$ 40 W m^{-1} for basalt, respectively, is distributed over 1 year (13.35 W m^{-1} granite and 8.22 W m^{-1} basalt) and each BHE of both fields with 20 BHEs and 6 BHEs are operated continuously over a period of 30 years, and following 30 years the ground temperature is observed as recovery phase (Table 6). Temperature values are observed starting from the middle of the field along the cross section, because the strongest cooling occurs at the center of field.

4.2.2. Results

Empirical heat extraction values are established to keep the temperature decrease in the subsurface in an acceptable range. For the multi-BHEs field studies, a cross section of the temperature change along the dashed line as depicted in Fig. 13a) and b) are plotted in Fig. 14a) and b) for all 4 scenarios at the end of the production period and subsequent 30th year of recovery phase after the operation, respectively. As can be seen in Fig. 14a), relative temperature difference of Scenarios 2 and 4 reach up to 15 K due to larger number of BHEs on the field. On the other hand, the specific heat extraction values given by VDI 4640 [31] provide optimum temperature drop in the ground for basalt and granite. However, temperature results shown in Fig. 14b) demonstrate that the temperature recovery of different geologies is not identical. The difference between the total amount of extracted heat and also different thermal parameters of basalt and granite can be account for the temperature difference between Scenarios 1–2 and 3–4 after 30 years recovery phase.

Only in conduction case, the optimum temperature decrease between scenarios may give a linear relationship between the specific heat extraction rate and the thermal conductivity of the ground. To investigate further, the thermal conductivity of basalt and granite versus the heat extraction rates given for those two scenarios are plotted and fitted with a linear regression curve. To validate the relationship, two corresponding points are matched from the middle of the linear curve as Case 1 and Case 2 (Fig. 15 the characteristics of which being reported in Table 7).

Number of BHEs remained identical as the previous Scenarios 2 and 4.

Comparison results shown in Fig. 16a) demonstrate that the relative temperature decrease between scenarios and generated cases are nearly optimum in the BHE field. This indicates that there is a linear relationship between heat extraction values and the thermal conductivity of the ground. The temperature difference after 30 years recovery shown in Fig. 13b) can be again account for the difference between the extracted total amount of heat of scenarios and different thermal parameters of media.

5. Conclusion

Analytical solutions of GSHP systems are preferable to have a better comprehension about the heat transfer system of the ground. Starting from the Green's function, which is a solution of

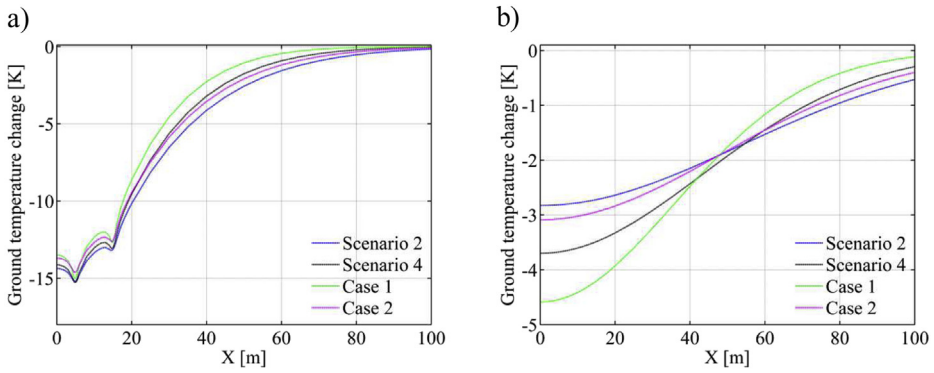

Fig. 16. Comparison results of scenarios and generated cases over distance at the depth of 50 m a) at the end of 30th year production period b) at the end of 30th year recovery period.

the conduction/advection/dispersion heat transfer in porous media, we deduced an analytical solution that provides temperature distribution around single and multi-BHEs for discontinuous heat extraction or storage. Axial effect and groundwater flow are considered. The proposed analytical solutions are validated with numerical code. Non-symmetric distribution of temperature plume is obtained due to advection and dispersion processes induced by the groundwater movement. In particular, thermal dispersion induces anisotropic thermal conduction that enhances the heat transfer in the direction of the flow. The new approach provides significantly shorter computation time compared to numerical simulation to obtain the required temperature results of a long-term production of GSHP systems and subsequent recovery period of the subsurface in given coordinates. On the other hand, this convenient tool may remarkably help for engineering applications to design and to plan multi-BHEs field easily under different hydro-geological conditions.

Those developed analytical solutions have been used to study sustainability and recovery aspects of BHE. The results of single BHE show that to use an optimum heat extraction value for BHE is not appropriate under different hydro-geological conditions, because the temperature drop of the ground rises with decreasing thermophysical properties of the subsurface. Moreover, to set an optimum heat extraction rate under any ground condition may cause larger impact on a multiple BHEs field. By using some empirical specific heat extraction rate values provided by VDI 4640, identical temperature impact in the subsurface under different geological conditions are observed after 30 years operation for different multi-BHEs fields. Afterwards, a best fit plot between thermal conductivity of the ground and the heat extraction rate demonstrate that the linear relationship can be used to determine an optimum heat extraction value for BHEs. However, the linear relationship is appropriate only if the volumetric heat capacity of medium is in a range of 2.5–3 MJ m^{-3} K^{-1} in conduction dominated heat transfer system.

The results of both single and multi-BHEs indicate that in case of only heating operations in only conduction dominated heat transfer system, the recovery period of the subsurface is not based on the duration of the production period, but depends on the total amount of heat that is extracted. In order to operate a BHE sustainable in a long-term, particularly multi-BHEs field, the recovery period shall be longer than the duration of production period. In fact, the re-operation of the system after a too short recovery phase may cause a decrease of the absolute temperature of the subsurface down to the freezing point of groundwater that can damage the backfilling material.

Acknowledgments

We thank the anonymous reviewers for their insightful comments, which have improved the quality of this work. Support for this work was partially provided by the financial support from Walloon Region in Belgium (GeoTherWal Project).

References

[1] L. Rybach, T. Mégel, W.J. Eugster, At what time scale are geothermal resources renewable?, in: Proceedings World Geothermal Congress 2000, Kyushu-tohoku, Japan, 2000.
[2] E. Barbier, Geothermal energy technology and current status: an overview, Renew. Sustain. Energy Rev. 6 (1–2) (2002) 3–65.
[3] L. Rybach, W.J. Eugster, Sustainability aspects of geothermal heat pumps, in: Proceedings 27th Workshop on Geothermal Reservoir Engineering, Standford University, Palo Alto, USA, 2002.
[4] S. Signorelli, Geoscientific Investigations for the Use of Shallow Low-enthalpy Systems, Doctoral Thesis, Swiss Federal Institute of Technology Zürich, Zürich, Switzerland, 2004.
[5] R. Curtis, W.J. Lund, B. Sanner, L. Rybach, G. Hellström, Ground source heat pumps – geothermal energy for anyone, anywhere: current worldwide activity, in: Proceedings World Geothermal Congress 2005, Antalya, Turkey, 2005.
[6] W.J. Lund, D.H. Freeston, T.L. Boyd, Direct application of geothermal energy: 2005 worldwide review, Geothermics 34 (2005) 691–727.
[7] M. O'Sullivan, A. Yeh, W. Mannington, Renewability of geothermal resources, Geothermics 39 (2010) 314–320.
[8] S. Lazzari, A. Priarone, E. Zanchini, Long-term performance of BHE (borehole heat exchanger) fields with negligible groundwater movement, Energy 35 (2010) 4966–4974.
[9] E. Zanchini, S. Lazzari, A. Priarone, Long-term performance of large borehole heat exchanger fields with unbalanced seasonal loads and groundwater flow, Energy 38 (2012) 66–77.
[10] P. Eskilson, Thermal Analysis of Heat Extraction Boreholes, Doctoral Thesis, University of Lund, Lund, Sweden, 1987.
[11] H.Y. Zeng, N.R. Diao, Z.H. Fang, A finite line-source model for boreholes in geothermal heat exchangers, Heat Transf. Asian Res. 31 (7) (2002) 558–567.
[12] M.G. Sutton, D.W. Nutter, R.J. Couvillion, A ground resistance for vertical borehole heat exchangers with groundwater flow, J. Energy Resour. Technol. 125 (3) (2003) 183–189.
[13] N. Diao, Q. Li, Z. Fang, Heat transfer in ground heat exchangers with groundwater advection, Int. J. Therm. Sci. 43 (12) (2004) 1203–1211.
[14] D. Marcotte, P. Pasquier, F. Sheriff, M. Bernier, The importance of axial effects for borehole design of geothermal heat-pump systems, Renew. Energy 35 (4) (2010) 763–770.
[15] Y. Man, H. Yang, N. Diao, J. Liu, Z. Fang, A new model and analytical solutions for borehole and pile ground heat exchangers, Int. J. Heat Mass Transf. 53 (13–14) (2010) 2593–2601.
[16] N. Molina-Giraldo, P. Bayer, P. Blum, K. Zhu, Z. Fang, A moving finite line source model to simulate borehole heat exchangers with groundwater advection, Int. J. Therm. Sci. 50 (2011) 2506–2513.
[17] J. Claesson, P. Eskilson, Conductive heat extraction by a deep borehole, thermal analysis and dimensioning rules, Energy 13 (6) (1988) 509–527.
[18] G. Hellström, Ground Heat Storage Thermal Analyses of Duct Storage Systems, I. Theory, Doctoral Thesis, University of Lund, Lund, Sweden, 1991.
[19] H.S. Carslaw, J.C. Jaeger, Conduction of Heat in Solids, second ed., Oxford University Press, New York, 1959.
[20] J. Claesson, T. Probert, Temperature Field Due to Time-dependent Heat Sources in a Large Rectangular Grid, Derivation of Analytical Solution, Technical Report, Svensk Kärnbränslehantering AB, Stockholm, Sweden, 1996.
[21] E. Zanchini, B. Pulvirenti, An analytical solution for the temperature field around a cylindrical surface subjected to a time dependent heat flux, Int. J. Heat Mass Transf. 66 (2013) 906–910.
[22] J.D. Deerman, S.P. Kavanaugh, Simulation of vertical U-tube ground-coupled heat pump systems using the cylindrical heat source solution, ASHRAE Trans. 97 (1) (1991) 287–295.
[23] S.P. Kavanaugh, K. Rafferty, Ground Source Heat Pumps: Design of Geothermal Systems for Commercial and Institutional Buildings, American Society of Heating, Refrigerating and Air-Conditioning Engineers, Atlanta, USA, 1997.
[24] S. Gehlin, Thermal Response Test - Method, Development and Evaluation, Doctoral Thesis, Luleå University of Technology, Luleå, Sweden, 2002.
[25] C. Yavuzturk, Modeling of Vertical Ground Loop Heat Exchangers for Ground Source Heat Pump Systems, Doctoral Thesis, Oklahoma State University, USA, 1999.
[26] M.A. Bernier, P. Pinel, R. Labib, R. Paillot, A multiple load aggregation algorithm for annual hourly simulations of GCHP systems, HVAC R Res. 10 (2004) 471–488.
[27] D. Marcotte, P. Pasquier, Fast fluid and ground temperature computation for geothermal ground-loop heat exchanger systems, Geothermics 37 (2008) 651–665.
[28] L. Lamarche, A fast algorithm for the hourly simulations of ground-source heat pumps using arbitrary response factors, Renew. Energy 34 (10) (2009) 2252–2258.
[29] A. Michopoulos, N. Kyriakis, A new energy analysis tool for ground source heat pump systems, Energy Build. 41 (2009) 937–941.
[30] A. Michopoulos, N. Kyriakis, The influence of a vertical ground heat exchanger length on the electricity consumption of the heat pumps, Renew. Energy 35 (2010) 1403–1407.
[31] N. Molina-Giraldo, P. Bayer, P. Blum, Evaluating the influence of thermal dispersion on temperature plumes from geothermal systems using analytical solutions, Int. J. Therm. Sci. 50 (2011) 1223–1231.
[32] G. de Marsily, Quantitative Hydrogeology, Academic Press, San Diego, California, 1986.
[33] J.W. Hopmans, J. Simunek, K.L. Bristow, Indirect estimation of soil thermal properties and water flux using heat pulse probe measurements: geometry and dispersion effects, Water Resour. Res. 38 (1) (2002) 1006.
[34] J. Constantz, Heat as a tracer to determine streambed water exchanges, Water Resour. Res. 44 (4) (2008).
[35] J.P. Sauty, A.C. Gringarten, H. Fabris, D. Thiery, A. Menjoz, P.A. Landel, Sensible energy storage in aquifers 2. Field experiments and comparison with theoretical results, Water Resour. Res. 18 (1) (1982) 253–265.
[36] S.P. Neuman, Universal scaling of hydraulic conductivities and dispersivities in geologic media, Water Resour. Res. 26 (8) (1990) 1749–1758.

[37] M. Xu, Y. Eckstein, Use of weighted least-squares method in evaluation of the relationship between dispersivity and field scale, Ground Water 33 (6) (1995) 905–908.
[38] D. Schulze-Makuch, Longitudinal dispersivity data and implications for scaling behavior, Ground Water 43 (3) (2005) 443–456.
[39] T. Metzger, Dispersion Thermique en Milieux Poreux: Caractérisation expérimentale par Technique Inverse, Doctoral Thesis (in French), Institut National Polytechnique de Lorraine (INPL), Nancy, 2002.
[40] COMSOL, COMSOL 4.2a, Multiphysics Modeling, Finite Element Analysis and Engineering Simulations Software, COMSOL Inc., Burglington, MA, USA, 2012.
[41] VDI-Richtlinie, Thermal Use of the Underground, Blatt 1, Verain Deutscher Ingenieure, VDI-Verlag, Düsseldorf, Germany, 2001.
[42] J. Hecht-Méndez, M. de Paly, M. Beck, P. Bayer, Optimization of energy extraction for vertical closed-loop geothermal systems considering groundwater flow, Energy Convers. Manag. 66 (2013) 1–10.
[43] VDI-Richtlinie, Thermal Use of the Underground, Blatt 2, Verain Deutscher Ingenieure, VDI-Verlag, Düsseldorf, Germany, 2001.
[44] H. Fujii, R. Itoi, J. Fujii, Y. Uchida, Optimizing the design of large-scale ground-coupled heat pump systems using groundwater and heat transport modeling, Geothermics 34 (2005) 347–364.
[45] T. Katsura, K. Nagano, S. Narita, S. Takeda, Y. Nakamura, A. Okamoto, Calculation algorithm of the temperatures for pipe arrangement of multiple ground heat exchangers, Appl. Therm. Eng. 29 (2009) 906–919.